Article

Polyelectrolytes Complex-Based Hydrogels Derived from Natural Polymers and Cannabinoids for Applications as Wound Dressing

Paula Rodriguez Gerpe [1], Sebastián D'Ippólito [2], Débora Nercessian [2,*], Micaela Ferrante [1], Vera A. Alvarez [1] and Jimena S. Gonzalez [1,*]

[1] Thermoplastic Composite Material Group (COMP), Institute of Materials Science and Technology (INTEMA), National University of Mar del Plata (UNMdP) and National Research Council (CONICET), Colón 10890, Mar del Plata 7600, Argentina; paulirodriguez1198@gmail.com (P.R.G.); micaela.ferrante@gmail.com (M.F.); alvarezvera@fi.mdp.edu.ar (V.A.A.)

[2] Biology of Cannabis Group, Institute of Biological Research (IIB) and Biology Department, National University of Mar del Plata (UNMdP) and National Research Council (CONICET), Funes 3250, Mar del Plata 7600, Argentina; dippolit@mdp.edu.ar

* Correspondence: dnercess@mdp.edu.ar (D.N.); jimena.gonzalez@fi.mdp.edu.ar (J.S.G.)

Abstract: This research work focuses on the development of an environmentally friendly wound dressing using natural polymers. The inclusion of cannabis in these hydrogels stems from its innovative potential in medicine, particularly for wound healing and pain relief. The hydrogels were prepared by a simple methodology using natural polysaccharides, and cannabis extract through electrostatic interactions and crosslinking with sodium tripolyphosphate (TPP). Several tests were carried out to analyze the morphological, physical, thermal, mechanical, barrier, and antimicrobial properties of these hydrogels. Different types of hydrogels were synthesized including chitosan- gum arabic hydrogel (ChiGA), hydrogel loaded with cannabis extract (ChiGACann), hydrogel crosslinked with TPP (ChiGATPP), and ChiGACann crosslinked with TPP (ChiGACannTPP). The impact of both cannabis extract and TPP crosslinking on the properties of chitosan hydrogels was investigated. The significant swelling capacity measured to the hydrogels, with ChiGACann exhibiting a 250–350% in physiological conditions, making them suitable for wound dressing applications due to their exudate absorption capacity. Antimicrobial activity evaluation demonstrated that the hydrogels acted as barriers against different microorganisms, with Gram-positive bacteria being more sensitive than Gram-negative bacteria. Mechanical testing showed improved mechanical properties in the presence of cannabis extract and TPP crosslinking (20–30 kPa of compression modulus). In conclusion, these results highlight the application of ChiGACann hydrogels as promising materials for manufacturing wound dressings.

Keywords: PEC; gum arabic; chitosan; hydrogel; cannabinoids; wound dressing

1. Introduction

The electrostatic attraction between the positively charged groups of cationic polyelectrolyte and the negatively charged groups of the other polyelectrolyte led to the formation of the polyelectrolyte complex (PEC). These charged groups could be acid (as the –COOH) or basic (as the $-NH_2$). Polyelectrolyte hydrogels are a particular class of hydrogel whose behavior is connected to the variation of pH in their immersed media [1].

Hydrogels are 3D-polymer networks with applications in various areas such as biomedicine, tissue engineering, drug delivery systems [2], pollutant adsorption systems [3], and so forth. They are capable of absorbing and retaining large amounts of aqueous solutions or physiologic fluids. Moreover, hydrogels show soft and rubbery consistency and low interfacial tension towards biological fluids making them excellent tissue replacement devices [4,5]

Polysaccharide-based gels have received particular attention in the biomedical field due to their biocompatibility, low toxicity, and biodegradability characteristics [2,6]. Common natural polysaccharides used for hydrogel synthesis are chitosan and gum arabic. Chitosan (Chi) is natural alkaline polysaccharide, which comes from the chemical treatment of the deacetylation of chitin. This polymer has several advantages, including anticoagulant features, wound healing promotion, and antimicrobial properties, among others [7]. On the other hand, gum arabic (GA) is an amorphous and nontoxic natural polysaccharide, being the most common exudate gum. Exudate gums are natural polysaccharides extensively used in different industrial applications because of their emulsifying and stabilizing features [8]. Both are weak opposite polyelectrolytes, and chitosan has a pKa of ~6.5, which means that at least a half of the macromolecules of chitosan present in chitosan are positively charged. Gum arabic is negatively charged at pH above 2.2, due to the deprotonation of the carboxylic groups on its glucuronic acid residues [9]. Thus, based on electrostatic interactions, they can form films, hydrogels, microgels, multilayer films, etc., with several biomedical applications [8,10–12]. Hydrogels can be prepared by ionic complexation, and many examples of these materials have been reported: for instance, PECs based on chitosan/alginate/hyaluronic acid crosslinked by genipin [13], alginate with chitosan [4], or a membrane of chitosan/pectin/gum arabic polyelectrolyte complex have been obtained and have potential in controlled drug release applications [14].

Cannabinoids and related active compounds derived from *Cannabis sativa* L. plants possess a variety of pharmacological properties. Some of these properties have been extensively studied, such as their role in chronic pain, anxiety, or treating convulsions. Other effects, like the antimicrobial properties of cannabis extracts, are well documented, but this knowledge has no application in medicine, industry, or agriculture [15,16]. In a recent literature review, the effects of cannabinoids on skin wound healing were summarized [17]. For instance, in vitro proliferation and wound closure tests showed that cannabis extract activated cell migration and proliferation, suggesting the activation of extracellular component remodeling [18]. In vivo studies indicated that mice with burn wounds treated with cannabis-based products experienced increased wound contraction and reduced epithelialization time [19]. In human patients, those with epidermolysis bullosa reported improved symptoms when treated with the cannabis-based product [20]. Taking into account this antimicrobial capacity together with the anti-inflammatory ability of cannabis, the addition of extracts to polymeric compounds allows the generation of new materials with health applications.

Hydrogels are an advancement in conventional wound dressings, offering not only high elasticity, permeability, and water absorption but also excellent biocompatibility and compatibility. Hydrogel-based wound dressings have shown great effectiveness in mitigating bacterial infections and have emerged as an effective treatment for wounds [21,22]. A recent study [23] reported that hydrogel formulated with cannabidiol-containing alginate demonstrated significant efficacy in promoting wound healing. The hydrogel was found to effectively control inflammation and promote collagen deposition and the formation of granulation tissue, as well as facilitate blood vessel formation. Additionally, this suggests that hemp-based hydrogels have the potential to inhibit skin aging processes and enhance the viability of skin cells. Furthermore, a recent study has indicated that hydrogels incorporating cannabis extracts have a positive impact on skin hydration [24]. Additionally, a commercial hydrogel containing cannabis, when evaluated in mice, resulted in decreased inflammation and fibrogenesis, as well as increased wound closure and re-epithelialization [25]. Several literature reviews highlight recent studies on cannabinoids, focusing on their effects on wound dressing or skin health [17,26–28].

In the present study, we examine the production of hydrogel based on polyelectrolyte complexes between gum arabic and chitosan and the influence of the cannabis extract in the hydrogel formation. The physico-chemical, morphological, and antimicrobial properties of the final structures are examined and shown herein. In addition, mechanical and water vapor transmission properties are evaluated for its possible application as wound dressing.

2. Materials and Methods

2.1. Materials

The hydrogels were prepared using chitosan derived from chitin, sourced from Glentham Life Sciences (Corsham, UK), and gum arabic from Biopack (Buenos Aires, Argentina), both used as received. Buffer solutions were made with Sodium Bicarbonate from Q.B.S Reactives Analytics and Acetic Acid water from Cicarelli (Santa Fe, Argentina), also used as received. Sodium tripolyphosphate from Q.B.S Reactives Analytics served as the crosslinking agent. The cannabis extract incorporated into the hydrogels was obtained from the female inflorescences of *Cannabis sativa* L. plants (see below).

2.2. Preparation of Hydrogels from Polyelectrolyte Complexes

The cannabis extract used to charge the hydrogels was obtained as reported in Vozza Berardo and colleagues [16] from the female inflorescences of *Cannabis sativa* L. plants of the collection of Biology of Cannabis group. Plants were cultivated under controlled conditions of light, humidity, and temperature in a grow chamber. Female inflorescences were dried at 18 °C and processed by mechanical disruption with ethanol at a ratio of 1:10 (*w/v*). Then, the solvent was eliminated by vacuum rotary evaporation at low temperature and cannabinoids (THC, CBD, and CBN) were identified and quantified by high-performance liquid chromatography (HPLC) in a SHIMADZU (Kyoto, Japan) Prominence chromatograph, with Liquid Chromatography LC Solution software (LCsolution versión 1.2, Shimadzu, Kyoto, Japan), low-pressure quaternary pump, diode array detector, and manual injector. We used a C18 column of 250 mm length, 4.5 mm diameter, and 5 μm particle size with a 0.7 mL/min flow. Solvents methanol and acetonitrile used in the mobile phase were of HPLC grade. The cannabinoids reference standards were from Cerilliant® (St. Louis, TX, USA).

The preparation of the hydrogels (Figure 1) took place in three steps. In the first stage, the homogenization process by dropwise addition of the aqueous solutions of chitosan (Chi) (5 mg/mL) and gum arabic (GA) (20 mg/mL) al pH = 4.5 [29]. The addition of the cannabis extract was carried out in the gum arabic solution. The second step was the obtention of a precipitate formed after centrifuging at 8000 rpm for 30 min. The last step involved the air-drying of the precipitates for 24 h using plastic molds.
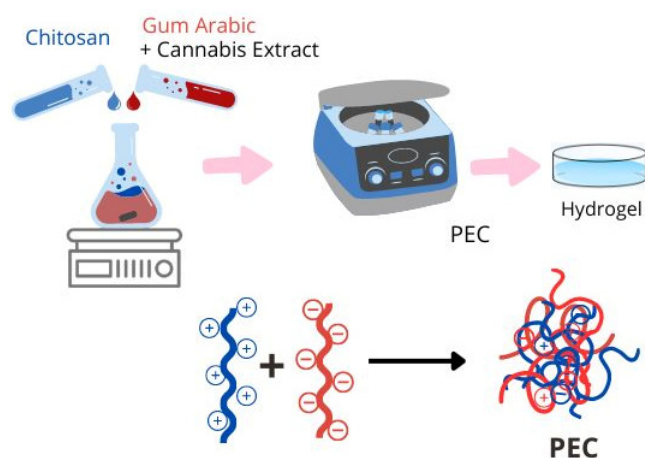
Figure 1. Obtaining scheme of polyelectrolyte complex.

Samples of hydrogels crosslinked with sodium tripolyphosphate (TPP) were subjected to two additional steps. First, the samples were immersed in a TPP solution (5 mg/mL) for 15 min as described in a published study [30]. Then, they were air-dried for 24 h using plastic molds.

The samples without TPP addition were named ChiGa and ChiGACann (with Cannabis Extract), and the samples with TPP solution were named ChiGATPP and ChiGACannTPP. As cannabis extraction was performed in ethanol, negative controls were obtained by

mixing same amounts of ethanol without cannabis with PECs solution containing Chi and GA (sample: ChiGAEt).

2.3. ζ Potential Studies

The test was conducted at pH 4.5 and 25 °C using the polymer solutions at the same concentration that those used to form the hydrogels: 5 mg/mL chitosan solution, 20 mg/mL gum arabic solution, and 20 mg/mL gum arabic with 5% *v/v* ethanol. Moreover, 5% *v/v* cannabis extract solution and TPP 5 mg/mL solution were also measured.

The test was made for triplicate and the zeta potential and standard deviation were obtained. The equipment employed was Horiba scientific, nano particle analyzer, SZ-100V2.

2.4. Thermogravimetric Analysis (TGA)

The thermogravimetric analysis data were recorded with a Shimadzu DTG-50 thermal analyzer (Kyoto, Japan). Samples were heated from room temperature to 800 °C at a heating rate of 10 °C per min under nitrogen atmosphere.

2.5. Fourier Transform Infrared (FTIR) Spectra

FTIR spectra of individual and crosslinked polymers were recorded in the range of 400–4000 cm^{-1} on a Thermo Scientific Nicolet 6700 spectrophotometer (Madison, WI, USA) with an attenuated total reflectance accessory (ATR). The raw materials, gum arabic and chitosan, were analyzed in powder form, the hydrogels in dry form. The cannabis extract was previously dried and analyzed as a powder.

2.6. Scanning Electron Microscopy (SEM)

The scanning electron microscopy measurements were performed on a Crossbeam 350 microscope from ZEISS (Oberkochen, Germany). The samples were previously frozen, lyophilized and cryo-fractured with liquid nitrogen.

2.7. Swelling Behavior Assay

First, the samples of each hydrogel were weighed completely dry (Wdry). Next, the gels were immersed in physiological solution at 37 °C, which simulates the physiological conditions of the human body. The mass of the sample was measured at different times (Wt), repeating this procedure until the samples began to disintegrate. The swelling percentage was calculated as follows.

$$\text{Swelling (\%)} = 100 * (\text{Wt} - \text{Wdry})/\text{Wdry} \tag{1}$$

2.8. Water Vapor Transmission Rate (WVTR)

The analyses were performed in a constant humidity chamber at 90% RH at 37 °C [31]. After 48 h, samples were removed from the chamber and the masses of the systems composed of hydrogel, container, distilled water and glue, which were previously weighed, were recorded.

The water vapor transmission rate index was calculated as follows

$$\text{WVTR (gm}^2 \times \text{h)} = 10^6 \times (\text{W0} - \text{W1})/(72 \times \text{A}) \tag{2}$$

where A is the area of the hydrogel in contact with vapor (mm^2) and W0 and W1 are the masses of the system (bottle, glue, water, and hydrogel) before and after placing them in the humidity chamber.

2.9. Compression Tests

The tests were carried out in static mode, at a temperature of 20 °C, using parallel plates and applying a compression of 10 mm. The initial force ranged from 50 nN up to 6000 nM, with a compression rate of 50 nN/min, until it reached a final force of 8000 nN, using Perkin Elmer DMA 7e equipment (Norwalk, CT, USA).

2.10. Antimicrobial Assays

Two different bacterial genera were used to analyze the antimicrobial effect of the hydrogels. The Gram-positive bacteria *Bacillus thurigensis* and the Gram-negative bacteria *Escherichia coli RP437* were grown in lysogeny broth (LB) broth (yeast extract 5 g/L, tryptone 10 g/L, and NaCl 10 g/L) with agitation at 37 °C for *E. coli* or 30 °C for *B. thurigensis*. Growth was followed by optical density at 600 nm (OD600) in a GeneQuantTM 1300 spectrophotometer (Chicago, IL, USA). Aliquots from cultures at exponential growth phase were inoculated into sterile culture media (new OD600 = 0.05) and then they were incubated with or without small pieces of the different hydrogels to be analyzed (ranging from 0.5 to 28 mg of each material) in order to obtain the possibility to test the effect along the entire growth curve. The effect of hydrogels on bacterial development was followed in time by measuring culture OD.

3. Results and Discussion

3.1. Morphological Characterization

Figure 2 depicts PECs ChiGA (a) and ChiGACann (b). As shown, both hydrogels exhibit a translucent and homogeneous appearance; however, ChiGACann acquires the characteristic bronze color of cannabis extract.
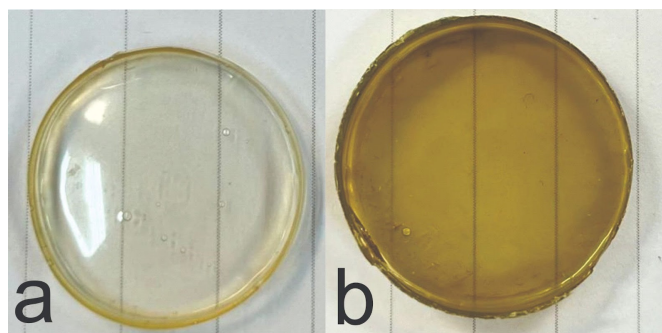
Figure 2. Photographs of PECs ChiGA (**a**) and ChiGACann (**b**).

Figure 3 displays a typical SEM image, revealing the porosity of the hydrogels. These pores are characterized as open and tiny, resembling the structure of a sponge. Specifically, ChiGA and ChiGACann exhibit pore sizes of 0.23 microns each; ChiGATPP has a pore size of 0.56 microns, and ChiGACannTPP features a pore size of 0.30 microns. Wall thicknesses were measured using ImageJ software v1.8.0 for the tested hydrogel samples. ChiGA exhibited a thickness of 621 nm, ChiGACann had 954 nm, ChiGACannTPP showed approximately 172 nm, and ChiGATPP had a thickness close to 400 nm.
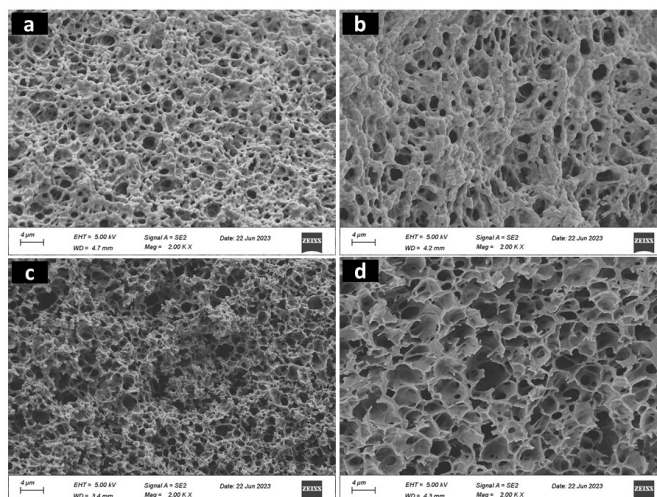

Figure 3. SEM images of (**a**) ChiGA, (**b**) ChiGACann, (**c**) ChiGACannTPP, (**d**) ChiGATPP samples.

One desirable characteristic of this type of material is that micropores are arranged in a structured way, so that they can absorb the wound exudates. Also, porosity is related to other sample characteristics such as pH, crosslinking density, and osmotic pressure [32]. As can be seen in Figure 3, the incorporation of cannabis extract and TPP positively influences the microstructure of the chitosan hydrogels, making them more organized.

3.2. Physico-Chemical Behavior

Zeta potential values were positive for chitosan and negative for gum arabic, as expected. The chitosan solution presented a potential of 22.5 ± 3.4 mV, while it was −12.7 ± 4.8 mV for the GA solution at obtaining conditions (pH 4.5). The addition of ethanol in GA solution does not seem to significantly change the potential of the solution (−10.4 ± 2.2 mV), as well as the addition of cannabis extract (−13.4 ± 1.4 mV). However, the zeta potential for the cannabis extract alone was −108.3 ± 29.8 mV and −6.3 ± 3.8 mV for the TPP solution. Taking this into account, the results may explain the beneficial effect of cannabis extract in the electrostatics interactions of polyelectrolytes. Although we expected that the TPP solution would allow for greater crosslinking in the hydrogel, we noted that its zeta potential is not as large, so its effect may not be noticeable. Further analysis was made to elucidate the mechanisms underlying these observations.

From Figure 4, thermogravimetric analysis (TGA) of Chi, two weight loss steps were detected. The first, which occurred at 54.3 °C, may be attributed to the loss of residual water, while the main decomposition occured at 301.6 °C. For GA, the decomposition temperature was found to be 311.5 °C.
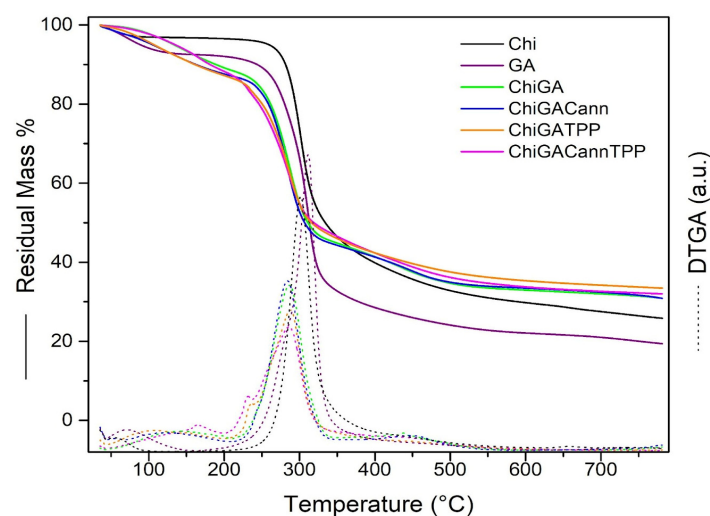

Figure 4. TGA curves of gels and raw polymers.

The thermograms of ChiGA, ChiGATPP, ChiGACann, and ChiGACannTPP exhibited three decomposition stages. The first decomposition stage in the range of 106.4–164.6 °C was attributed to the loss of bound water. The second, occurring between 283.7–286 °C, was associated with the dehydration and decarboxylation of the polymers. The third decomposition stage in the range of 434.2–451 °C resulted from the degradation of residual polymer. The addition of cannabis extract and crosslinking with TPP did not yield significant changes. The hydrogels exhibit a similar decomposition temperature range and demonstrate good thermal resistance, which is a positive indicator for their potential use in biomedical applications [33].

The FTIR spectra of GA, Chi, cannabis extract, ChiGA, ChiGATPP, ChiGACann, and ChiGACannTPP are depicted in Figure 5. The primary characteristic peaks of GA include 1021 cm^{-1} (C–O stretch), 1598 cm^{-1} (C–O stretch and N–H bending), 2898 cm^{-1} (C–H stretch), and 3322 cm^{-1} (O–H stretch). For chitosan, key peaks were observed at 1021 cm^{-1} (C-O stretch for amino groups), 1419 cm^{-1} (CH$_2$ bending), 1560 cm^{-1} (N-H stretch for

amino groups), 1655 cm^{-1} (absorbance of C=O), and 3291 cm^{-1} (O-H N-H stretch). In the cannabis extract, major peaks were identified at 1118 cm^{-1} (C-O stretch), 1563 cm^{-1} (C-H stretch of aliphatic groups), 1614 cm^{-1} (C=C stretch), and 2925 cm^{-1} (O-H stretch).
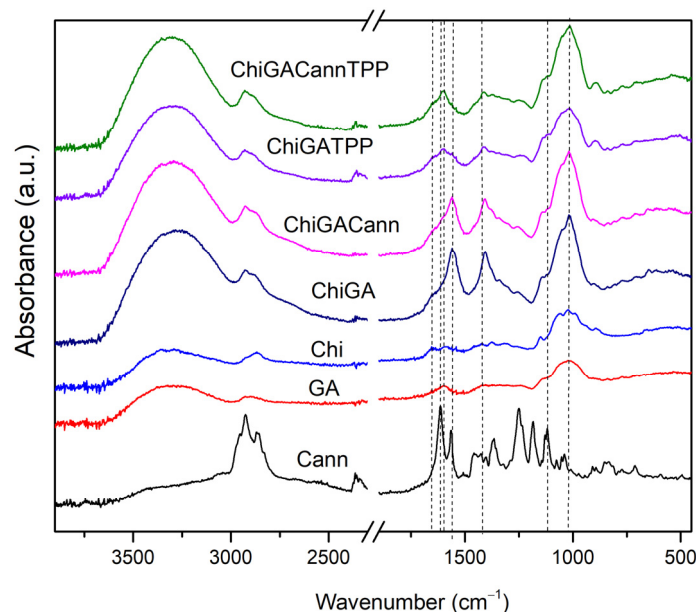
Figure 5. FTIR spectra of PECs and raw materials.

Figure 5 displays spectroscopies of all hydrogels revealing significant shifts in the 1400 cm^{-1} to 1600 cm^{-1} range. This corresponds to the carboxyl–amide region, involving the carboxyl groups of gum arabic and the amine groups of chitosan, indicating interaction between the biopolymers in the complexes [29,34]. In the case of polymers, an analysis of the intramolecular OH stretching mode in the spectral range of 2700–3900 cm^{-1} and in different conditions could be reveal more information about the interactions between them [35,36]

Upon incorporating cannabis extract into chitosan and gum arabic hydrogels, characteristic bands of the extract (2925 cm^{-1}, 1614 cm^{-1}, 1563 cm^{-1}, and 1118 cm^{-1}) appear in ChiGACann and ChiGACannTPP samples (Figure 5). Some peaks of the cannabis extract shift in ChiGACann and ChiGACannTPP due to molecular interaction with chitosan [33] and confirming interactions between the components of the polymers.

3.3. Swelling Behavior

Figure 6 shows the swelling behavior of ChiGA, ChiGACann, ChiGATPP, ChiGACan-nTPP, and ChiGAEt (with 5% *v/v* ethanol). We expected that the hydrogels with higher crosslinking would present lower swelling rates, but all samples displayed similar trends, with an exponential increase in swelling during the first hour. Swelling percentage is inversely proportional to the degree of crosslinking, indicating that higher crosslinking results in lower swelling [24].

All samples swelled in physiological conditions at 37 °C, and the swelling rates reached values around 250–350%. However, after 24 h, all hydrogels started to disintegrate; this was a limitation regarding the duration of the study, but taking into account the potential application of the hydrogels as wound dressings, we considered that one day would be enough, since the hydrogels would be replaced after this time.
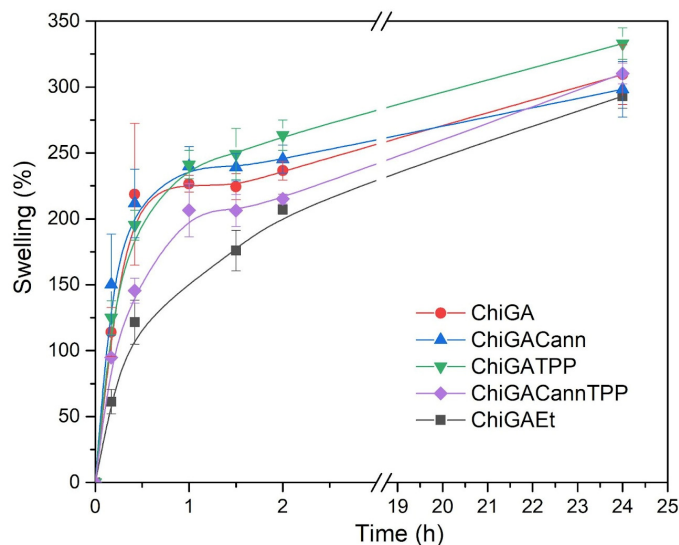
Figure 6. Swelling behavior of gels.

3.4. Mechanical Behavior

Stress–strain curves were generated for the four gels analyzed in this study: ChiGA, ChiGATPP, ChiGACann, and ChiGACannTPP. Figure 7 shows four analyzed samples. The mechanical properties of compression assay are shown in Table 1.
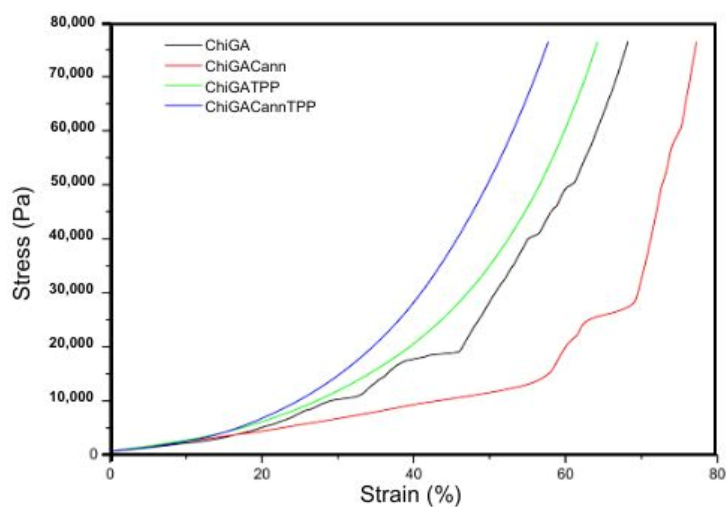

Figure 7. Stress–strain curves of compression test for the gels.

Table 1. Compression test properties.

Sample	ChiGA	ChiGACann	ChiGATPP	ChiGACannTPP
Compression Modulus (Pa)	$30{,}390 \pm 8$	$20{,}894 \pm 2$	$22{,}842 \pm 4664$	$30{,}619 \pm 1266$
Compression Resistant (Pa)	$10{,}033 \pm 2$	$16{,}140 \pm 3$	$76{,}387 \pm 1$	$76{,}389 \pm 6$
Strain (%)	25.42 ± 0.28	56.81 ± 2.63	60.98 ± 3.22	57.36 ± 0.35

The two-step stress–strain behavior in hydrogels can be attributed to their unique dual-network structure and water content. At low strains, the hydrogel deforms mainly through the extension of the polymer chains in the soft network. The presence of water allows these chains to move and reorient easily, leading to a relatively low and constant stress response. As the strain increases, the soft network becomes fully extended, and the stiff network starts to bear the load. This transition causes a significant increase in

stress, leading to the second step in the curve. The stiffer network resists deformation more strongly, resulting in a steeper slope in the stress–strain curve [37].

It is important to note that the compression modulus for each gel varied: ChiGA exhibited 30.390 kPa, ChiGACann exhibited 20.894 kPa, ChiGATPP showed 22.842 kPa, and ChiGACannTPP showed 30.619 kPa. These results indicate that hydrogels containing cannabis extract exhibit higher intrinsic elasticity compared to the other samples [24].

While the maximum strain trends are similar for ChiGACann, ChiGACannTPP, and ChiGATPP (55–65%), ChiGA differs with a strain value of less than 25%. The crosslinking process significantly enhances the mechanical properties, although it is noteworthy that the resulting gels, once dried, show increased brittleness [38].

3.5. Water Vapor Transmission Rate (WVTR)

In an ideal dressing, WVTR is expected to fall within a specific range between 8.33 and 10.42 g/m^2.h to promote wound healing [33]. The vapor permeability varies across hydrogels: ChiGA is 3 $g/m^2 \cdot h$, ChiGATPP is 3.9 $g/m^2 \cdot h$, ChiGACann is 5.1 $g/m^2 \cdot h$, and ChiGACannTPP is 2.7 $g/m^2 \cdot h$. Among all evaluated hydrogels, the cannabis-loaded hydrogel demonstrates the highest rate throughout the trial and approaches the desired level.

3.6. Antimicrobial Testing

Once analyzed, the mechanical and physico-chemical properties of the obtained hydrogels, their antimicrobial activity was assessed on *Bacillus thuringiensis*, (Gram-positive) and *Escherichia coli* (Gram-negative) bacteria. While these bacteria may not typically be found in wound infections, they were selected as they are model microorganisms of genera that include pathogenic species affecting animal and human health, including skin infections. Samples containing different concentrations of cannabis extract in the hydrogels as well as different amounts of hydrogels were incubated with bacterial cultures to identify the best combination needed to achieve 50% growth inhibition (Figure 8). For *Bacillus thuringiensis* the initial assays were performed with 28 mg of each hydrogel, which resulted in complete growth inhibition. Then, low amounts were tested, being the combination of 0.5 mg of hydrogel containing 0.08 mg of cannabis extract, the one chosen to continue the analysis. A 50% growth inhibition was achieved when the polymer tested was ChiGACannTPP. Interestingly, the same amount of polymer inhibited 100% bacterial growth when the hydrogel was ChiGACann (without the TPP crosslinker), indicating that the TPP trapped the active compounds, thus reducing their availability (Figure 9). When the bacterial culture tested was *Escherichia coli*, the antimicrobial activity was achieved with higher amounts of hydrogel with a higher concentration of cannabis extract (28 mg of hydrogel containing 0.12 mg/mg hydrogel) (Figure 8); therefore, the next assays were performed with those conditions (Figure 10). As a result of all these trials, a 50% growth reduction was obtained when using 0.04 mg cannabis extract in a 3 mL culture volume (i.e., 0.013 mg/mL) for Gram-positive bacteria and using 3.36 mg cannabis extract in a 3 mL culture volume (i.e., 1.12 mg/mL) for Gram-negative bacteria. These results are consistent with previous works reporting that Gram-negative microorganisms are more resistant to cannabis extracts [39,40].

It is important to note that hydrogels also contain chitosan, which is a known antimicrobial agent, but in the structures performed in this work, this effect was less evident than the observed for the materials containing both chitosan and cannabis (Figures 8–10), suggesting a synergistic activity. This positive association was also observed for the antifungal activity of cannabis loaded lipidic particles coated with chitosan [41]. In summary, cannabis-loaded hydrogels exhibit a pronounced and dose-dependent antimicrobial effect, more noticeable on *Bacillus thuringiensis* than on *Escherichia coli*.
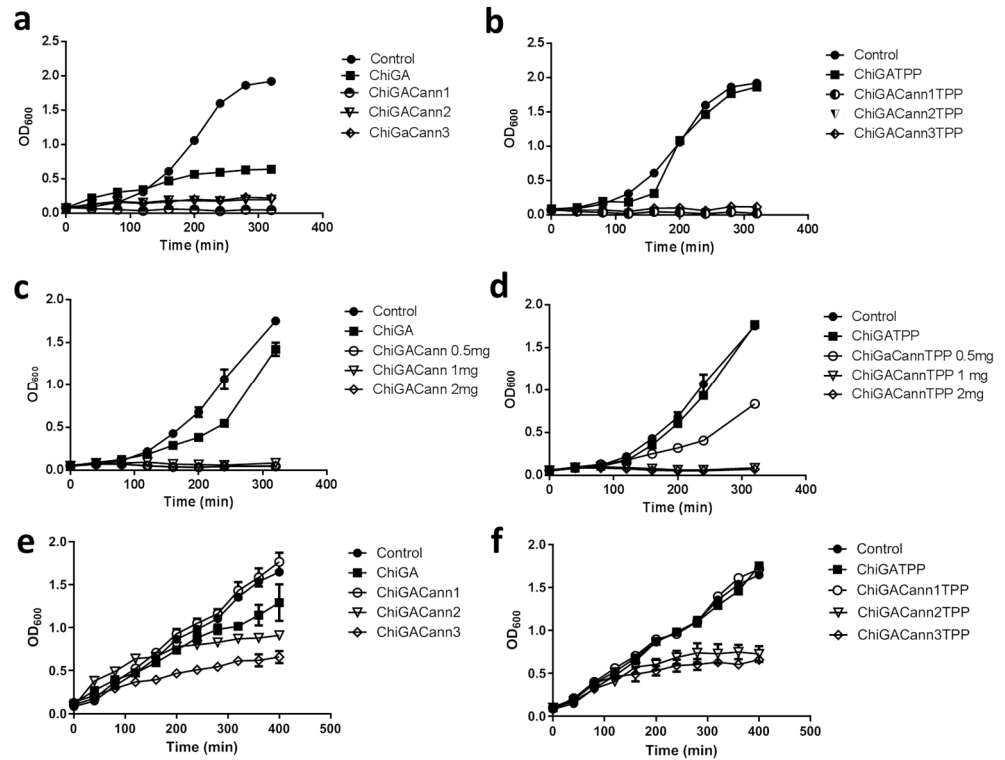
Figure 8. Effect of different amounts of hydrogels containing different concentrations of cannabis extract on bacterial growth development. (**a**–**d**): *B. thuringiensis*; (**e**,**f**): *E. coli*. (**a**) Amounts of 28 mg of hydrogels without TPP and (**b**) hydrogels with TPP. Cannabis concentration: Cann1 = 0.08 mg cannabis extract/mg hydrogel; Cann2 = 0.12 mg cannabis extract/mg hydrogel; Cann3 = 0.21 mg cannabis extract/mg hydrogel. (**c**,**d**) Amounts of 0.5, 1, or 2 mg of each hydrogel with cannabis extracts at concentration 1 (0.08 mg/mg hydrogel), without (**c**) or with (**d**) TPP. (**e**,**f**) Amounts of 28 mg of each hydrogel, (**e**) without and (**f**) with TPP. Each value is the mean ± SD of, at least, three independent experiments.
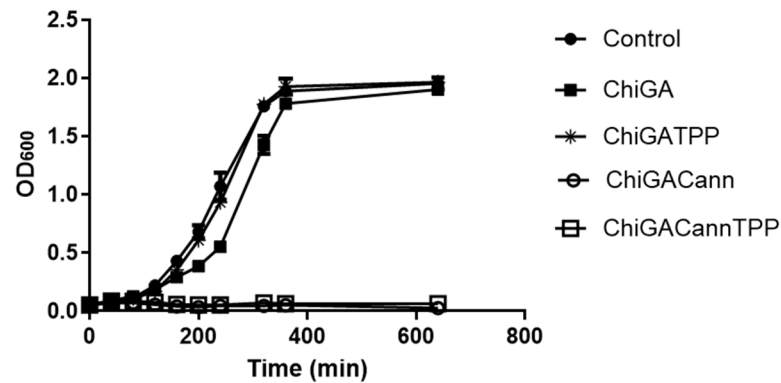
Figure 9. Effect of hydrogels (0.5 mg) with or without cannabis extract (0.08 mg/mg hydrogel) on growth development of *B. thuringiensis*. Each value is the mean ± SD of, at least, three independent experiments.
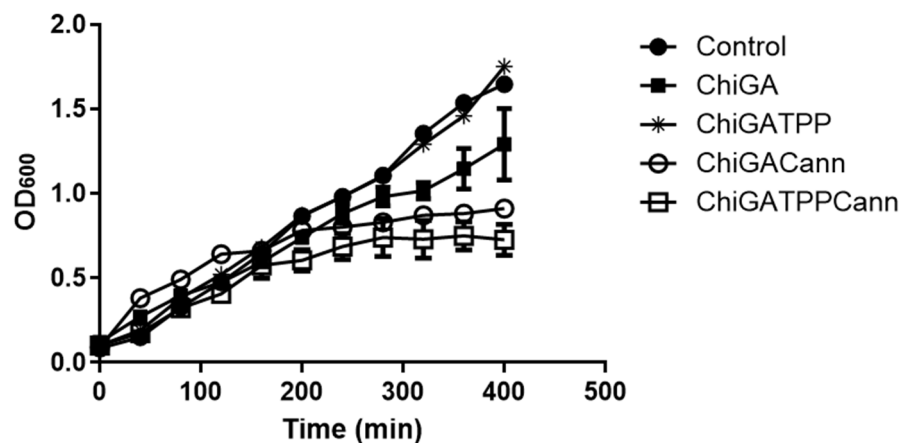
Figure 10. Effect of hydrogels (28 mg) with or without cannabis extract (0.12 mg/mg hydrogel) on growth development of *E. coli*. Each value is the mean ± SD of, at least, three independent experiments.

4. Conclusions

This study successfully developed and characterized hybrid materials containing chitosan, gum arabic, and cannabis extract that exert synergistic antimicrobial activity against Gram-positive and -negative bacteria, this effect being highest against Gram-positive microorganisms. The easy preparation and integration into the hydrogel materials make cannabis extracts promising additives to functional biomaterials. The physicochemical and initial biological properties of the hydrogels showed promising results for potential application as wound dressings. However, further studies, including in vivo testing and long-term stability assessments, are needed to fully evaluate their suitability.

Future research on cannabis-infused polyelectrolyte complex hydrogels should focus on optimizing the hydrogel composition, exploring a wider range of cannabinoids, and conducting in vivo testing to confirm efficacy and safety. Additionally, enhancing the antimicrobial and anti-inflammatory properties, assessing environmental impact and sustainability, and investigating applications beyond wound care could significantly advance their biomedical utility. Long-term stability and practical storage conditions will also be crucial for ensuring the reliability and commercial viability of these hydrogels.

Institutional Review Board Statement: Not applicable.

Data Availability Statement: Datasets generated during the current study are available from the corresponding author upon reasonable request.

Conflicts of Interest: The authors declare no conflicts of interest.

References

1. Meka, V.S.; Sing, M.K.G.; Pichika, M.R.; Nali, S.R.; Kolapalli, V.R.M.; Kesharwani, P. A comprehensive review on polyelectrolyte complexes. *Drug Discov. Today* **2017**, *22*, 1697–1706. [CrossRef] [PubMed]
2. Ferrante, M.; Alvarez, V.A.; Gende, L.B.; Guerrieri, D.; Chuluyan, E.; Gonzalez, J.S. Polyelectrolyte complexes hydrogels based on chitosan/pectin/NaCl for potentially wound dressing: Development, characterization, and evaluation. *Colloid Polym. Sci.* **2024**, *302*, 1231–1245. [CrossRef]
3. Areal, M.P.; Arciniegas, M.L.; Horst, F.; Lassalle, V.; Sánchez, F.H.; Alvarez, V.A.; Gonzalez, J.S. Water Remediation: PVA-Based Magnetic Gels as Efficient Devices to Heavy Metal Removal. *J. Polym. Environ.* **2018**, *26*, 3129–3138. [CrossRef]
4. Candia, C.; Gallardo-Moya, D.; Guerrero, J.; Leal, D.; Mansilla, A.; Martínez-Gómez, F.; Matsuhiro, B.; Yáñez-S, M. Characterization of alginate from Antarctic *Himantothallus grandifolius* (Phaeophyceae) and preparation of polyelectrolyte complexes with chitosan. *J. Appl. Polym. Sci.* **2023**, *140*, e54688. [CrossRef]
5. Hoffman, A.S. Hydrogels for biomedical applications. *Adv. Drug Deliv. Rev.* **2012**, *64*, 18–23. [CrossRef]
6. Safarzadeh Kozani, P.; Safarzadeh Kozani, P.; Hamidi, M.; Valentine Okoro, O.; Eskandani, M.; Jaymand, M. Polysaccharide-based hydrogels: Properties, advantages, challenges, and optimization methods for applications in regenerative medicine. *Int. J. Polym. Mater. Polym. Biomater.* **2022**, *71*, 1319–1333. [CrossRef]
7. Che, X.; Zhao, T.; Hu, J.; Yang, K.; Ma, N.; Li, A.; Sun, Q.; Ding, C.; Ding, Q. Application of Chitosan-Based Hydrogel in Promoting Wound Healing: A Review. *Polymers* **2024**, *16*, 344. [CrossRef]
8. De Souza, A.G.; Cesco, C.T.; de Lima, G.F.; Artifon, S.E.S.; Rosa, D.d.S.; Paulino, A.T. Arabic gum-based composite hydrogels reinforced with eucalyptus and pinus residues for controlled phosphorus release. *Int. J. Biol. Macromol.* **2019**, *140*, 33–42. [CrossRef]
9. Weinbreck, F.; Tromp, R.H.; de Kruif, C.G. Composition and Structure of Whey Protein/Gum Arabic Coacervates. *Biomacromolecules* **2004**, *5*, 1437–1445. [CrossRef]
10. Mota, H.P.; Fajardo, A.R. Development of superabsorbent hydrogel based on Gum Arabic for enhanced removal of anxiolytic drug from water. *J. Environ. Manag.* **2021**, *288*, 112455. [CrossRef]
11. Milenkova, S.; Zahariev, N.; Ambrus, R.; Pilicheva, B.; Marudova, M. A Study on the Stoichiometry of Casein/Chitosan Gel Complexes as a Delivery System for Quercetin. *Appl. Sci.* **2023**, *13*, 10868. [CrossRef]
12. Gerola, A.P.; Silva, D.C.; Matsushita, A.F.Y.; Borges, O.; Rubira, A.F.; Muniz, E.C.; Valente, A.J.M. The effect of methacrylation on the behavior of Gum Arabic as pH-responsive matrix for colon-specific drug delivery. *Eur. Polym. J.* **2016**, *78*, 326–339. [CrossRef]
13. Meng, X.; Lu, Y.; Gao, Y.; Cheng, S.; Tian, F.; Xiao, Y.; Li, F. Chitosan/alginate/hyaluronic acid polyelectrolyte composite sponges crosslinked with genipin for wound dressing application. *Int. J. Biol. Macromol.* **2021**, *182*, 512–523. [CrossRef] [PubMed]
14. Tsai, R.Y.; Chen, P.W.; Kuo, T.Y.; Lin, C.M.; Wang, D.M.; Hsien, T.Y.; Hsieh, H.J. Chitosan/pectin/gum Arabic polyelectrolyte complex: Process-dependent appearance, microstructure analysis and its application. *Carbohydr. Polym.* **2014**, *101*, 752–759. [CrossRef]
15. Schofs, L.; Sparo, M.D.; Sánchez Bruni, S.F. The antimicrobial effect behind Cannabis sativa. *Pharmacol. Res. Perspect.* **2021**, *9*, e00761. [CrossRef]
16. Vozza Berardo, M.E.; Mendieta, J.R.; Villamonte, M.D.; Colman, S.L.; Nercessian, D. Antifungal and antibacterial activities of *Cannabis sativa* L. resins. *J. Ethnopharmacol.* **2024**, *318*, 116839. [CrossRef]
17. Parikh, A.C.; Jeffery, C.S.; Sandhu, Z.; Brownlee, B.P.; Queimado, L.; Mims, M.M. The effect of cannabinoids on wound healing: A review. *Health Sci. Rep.* **2024**, *7*, e1908. [CrossRef]
18. Styrczewska, M.; Kostyn, A.; Kulma, A.; Majkowska-Skrobek, G.; Augustyniak, D.; Prescha, A.; Czuj, T.; Szopa, J. Flax Fiber Hydrophobic Extract Inhibits Human Skin Cells Inflammation and Causes Remodeling of Extracellular Matrix and Wound Closure Activation. *Biomed Res. Int.* **2015**, *2015*, 862391. [CrossRef]
19. Zheng, J.-L.; Yu, T.-S.; Li, X.-N.; Fan, Y.-Y.; Ma, W.-X.; Du, Y.; Zhao, R.; Guan, D.-W. Cannabinoid receptor type 2 is time-dependently expressed during skin wound healing in mice. *Int. J. Legal Med.* **2012**, *126*, 807–814. [CrossRef]
20. Chelliah, M.P.; Zinn, Z.; Khuu, P.; Teng, J.M.C. Self-initiated use of topical cannabidiol oil for epidermolysis bullosa. *Pediatr. Dermatol.* **2018**, *35*, e224–e227. [CrossRef]
21. Sun, Y.; Li, D.; Yu, Y.; Zheng, Y. Insights into the Role of Natural Polysaccharide-Based Hydrogel Wound Dressings in Biomedical Applications. *Gels* **2022**, *8*, 646. [CrossRef] [PubMed]
22. Zhong, Y.; Xiao, H.; Seidi, F.; Jin, Y. Natural Polymer-Based Antimicrobial Hydrogels without Synthetic Antibiotics as Wound Dressings. *Biomacromolecules* **2020**, *21*, 2983–3006. [CrossRef] [PubMed]
23. Zheng, Z.; Qi, J.; Hu, L.; Ouyang, D.; Wang, H.; Sun, Q.; Lin, L.; You, L.; Tang, B. A cannabidiol-containing alginate based hydrogel as novel multifunctional wound dressing for promoting wound healing. *Biomater. Adv.* **2022**, *134*, 112560. [CrossRef]
24. Zagórska-Dziok, M.; Bujak, T.; Ziemlewska, A.; Nizioł-Łukaszewska, Z. Positive effect of cannabis sativa l. Herb extracts on skin cells and assessment of cannabinoid-based hydrogels properties. *Molecules* **2021**, *26*, 802. [CrossRef] [PubMed]
25. Zhao, C.; Dong, Y.; Liu, J.; Cai, H.; Li, Z.; Sun, X.; Yin, W.; Ma, J.; Liu, H.; Li, S. An enzyme-responsive Gp1a-hydrogel for skin wound healing. *J. Biomater. Appl.* **2021**, *36*, 714–721. [CrossRef] [PubMed]
26. Filipiuc, S.-I.; Neagu, A.-N.; Uritu, C.M.; Tamba, B.-I.; Filipiuc, L.-E.; Tudorancea, I.M.; Boca, A.N.; Hâncu, M.F.; Porumb, V.; Bild, W. The Skin and Natural Cannabinoids–Topical and Transdermal Applications. *Pharmaceuticals* **2023**, *16*, 1049. [CrossRef]
27. Yoo, E.H.; Lee, J.H. Cannabinoids and Their Receptors in Skin Diseases. *Int. J. Mol. Sci.* **2023**, *24*, 16523. [CrossRef]

28. Sivesind, T.E.; Maghfour, J.; Rietcheck, H.; Kamel, K.; Malik, A.S.; Dellavalle, R.P. Cannabinoids for the Treatment of Dermatologic Conditions. *JID Innov.* **2022**, *2*, 100095. [CrossRef]

29. Espinosa-Andrews, H.; Ba, J.G.; Cruz-Sosa, F.; Vernon-Carter, E.J. Gum Arabic—Chitosan Complex Coacervation. *Biomacromolecules* **2007**, *8*, 1313–1318. [CrossRef]

30. Dureja, H.; Tiwary, A.K.; Gupta, S. Simulation of skin permeability in chitosan membranes. *Int. J. Pharm.* **2001**, *213*, 193–198. [CrossRef]

31. Kokabi, M.; Sirousazar, M.; Hassan, Z.M. PVA-clay nanocomposite hydrogels for wound dressing. *Eur. Polym. J.* **2007**, *43*, 773–781. [CrossRef]

32. Ferrante, M.; Álvarez, V.A.; Narain, R.; Ounkaew, A.; Gonzalez, J.S. Enhancing the Properties of Chitosan—Pectin Hydrogels with Cellulose Nanowhiskers for Potential Applications in Wound Dressings. *Macromol. Chem. Phys.* **2024**, *225*, 2400088. [CrossRef]

33. Chelminiak-Dudkiewicz, D.; Smolarkiewicz-Wyczachowski, A.; Mylkie, K.; Wujak, M.; Mlynarczyk, D.T.; Nowak, P.; Bocian, S.; Goslinski, T.; Ziegler-Borowska, M. Chitosan-based films with cannabis oil as a base material for wound dressing application. *Sci. Rep.* **2022**, *12*, 18658. [CrossRef] [PubMed]

34. Espinosa-Andrews, H.; Sandoval-Castilla, O.; Vázquez-Torres, H.; Vernon-Carter, E.J.; Lobato-Calleros, C. Determination of the gum Arabic-chitosan interactions by Fourier Transform Infrared Spectroscopy and characterization of the microstructure and rheological features of their coacervates. *Carbohydr. Polym.* **2010**, *79*, 541–546. [CrossRef]

35. Caccamo, M.T.; Magazù, S. Thermal restraint on PEG-EG mixtures by FTIR investigations and wavelet cross-correlation analysis. *Polym. Test.* **2017**, *62*, 311–318. [CrossRef]

36. Caccamo, M.T.; Mavilia, G.; Mavilia, L.; Lombardo, D.; Magazù, S. Self-assembly processes in hydrated montmorillonite by FTIR investigations. *Materials* **2020**, *13*, 1100. [CrossRef]

37. Li, L.; Scheiger, J.M.; Levkin, P.A. Design and Applications of Photoresponsive Hydrogels. *Adv. Mater.* **2019**, *31*, 1807333. [CrossRef]

38. Yang, C.; Xu, L.; Zhou, Y.; Zhang, X.; Huang, X.; Wang, M.; Han, Y.; Zhai, M.; Wei, S.; Li, J. A green fabrication approach of gelatin/CM-chitosan hybrid hydrogel for wound healing. *Carbohydr. Polym.* **2010**, *82*, 1297–1305. [CrossRef]

39. Karas, J.A.; Wong, L.J.M.; Paulin, O.K.A.; Mazeh, A.C.; Hussein, M.H.; Li, J.; Velkov, T. The Antimicrobial Activity of Cannabinoids. *Antibiotics* **2020**, *9*, 406. [CrossRef]

40. Van Klingeren, B.; ten Ham, M. Antibacterial activity of Δ9-tetrahydrocannabinol and cannabidiol. *Antonie Van Leeuwenhoek* **1976**, *42*, 9–12. [CrossRef]

41. Menossi, M.; Tejada, G.; Colman, S.L.; Nercessian, D.; Mendieta, J.R.; Islan, G.A.; Alvarez, V.A. Cannabis extract-loaded lipid and chitosan-coated lipid nanoparticles with antifungal activity. *Colloids Surf. A Physicochem. Eng. Asp.* **2024**, *685*, 133207. [CrossRef]